

Figure 1. C-176 inhibits cyclic di-nucleotide (CDN) mediated STING activation.

Inhibition of STING and TBK1 phosphorylation occurs in BV2 microglia-like cells pre-treated for 30 minutes with STING inhibitor C-176 and treated for 8 hours with 10-20 μg of c-di-GMP. (A) Protein expression analysed by western blot. Densitometric analysis (B-C) was performed to quantitate expression of p-STING relative to STING and p-TBK1 relative to TBK1. Protein expression was measured as ratio of band intensity and β -actin loading control. The expression of p-STING (B) and p-TBK1 (C) was made relative to total protein expression of STING and TBK1 respectively. All data is expressed as mean \pm SEM. STING phosphorylation was significantly increased following treatment with 10 $\mu\text{g/mL}$ ($p=0.010$) and 20 $\mu\text{g/mL}$ ($p<0.0001$) of c-di-GMP compared to untreated vehicle. Treatment with 2 μM C-176 completely ablated c-di-GMP induced phosphorylation of STING. $n = 5$. Significance determined by two-way ANOVA followed by a Bonferroni's multiple comparison test within each dose of C-176. * $p<0.05$, ** $p<0.01$, *** $p<0.001$, **** $p<0.0001$

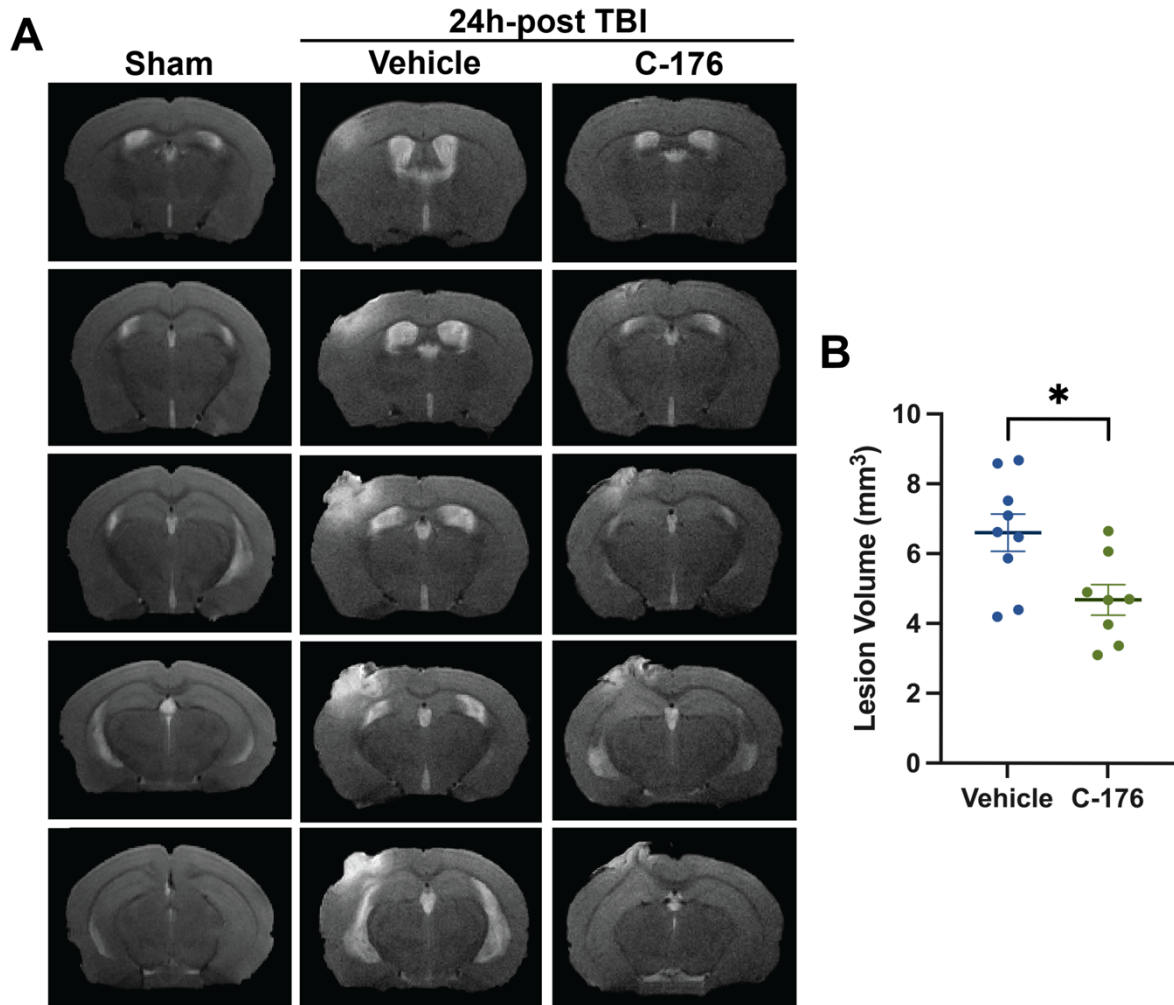


Figure 2. Administration of C-176 reduces TBI-induced brain lesion

MRI T2 images from C57BL/6 mice showing TBI lesion 24h-post injury (A). Mild TBI was modelled using a controlled cortical impactor. 30-minutes post-TBI, mice were intravenously administered a vehicle or C-176. Sham mice underwent identical surgery omitting the TBI. Mice administered C-176 post-TBI had significantly reduced lesion volumes 24h after injury (* $p=0.01$) (B). Data represents mean \pm SEM, $n=8-9$ animals per group.

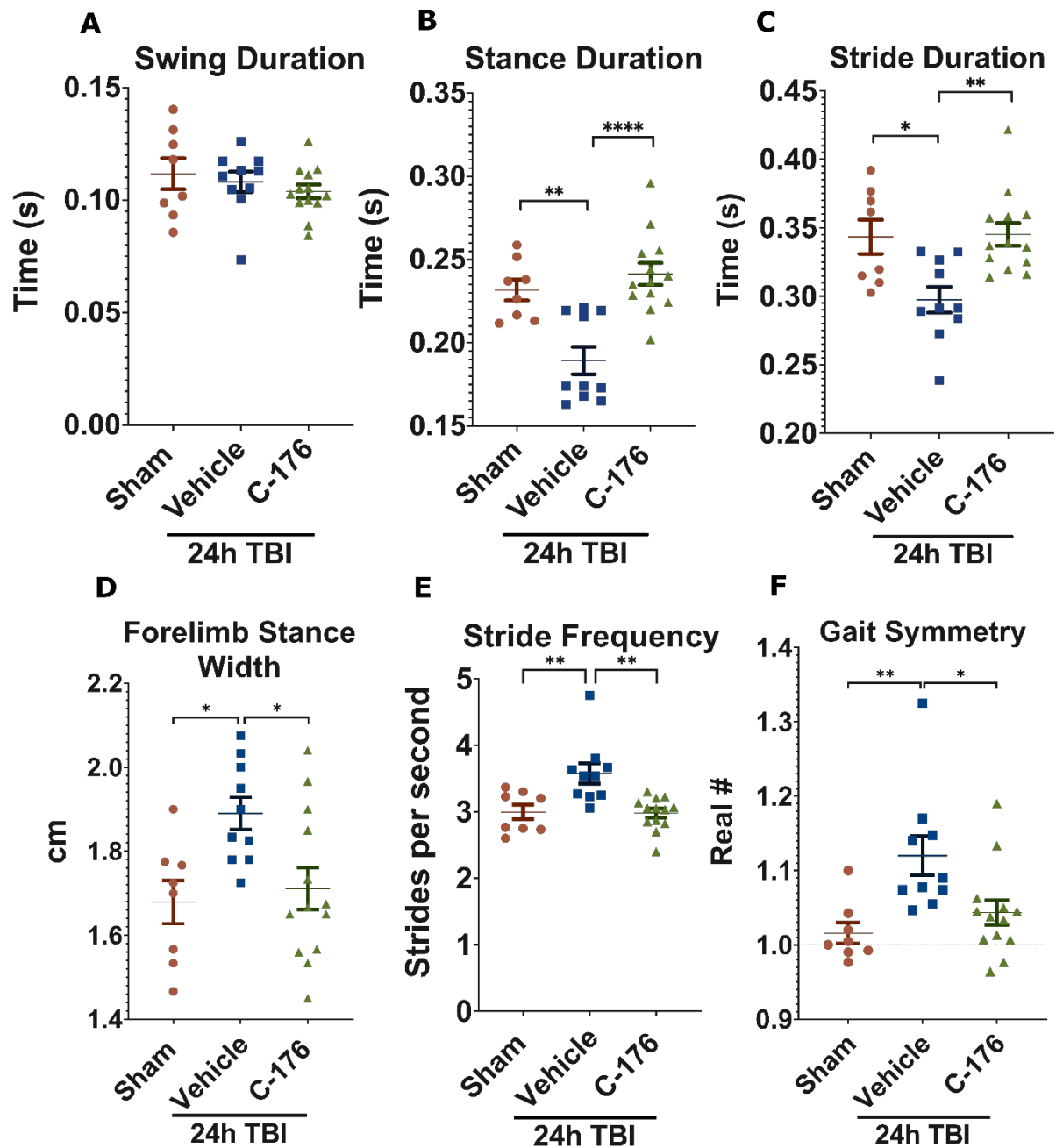


Figure 3. C-176 significantly improves left forelimb gait deficits 24h post-TBI.

Quantitative temporal gait parameters of mice were measured using DigiGait™ imaging and analysis software 24h after 1.5mm impact CCI surgery (TBI) and no impact (sham). No change in (A) swing duration was observed. Significant improvements found in (B) stance ($p < 0.0001$) and (C) stride duration ($p = 0.0032$), (D) stride frequency ($p = 0.0011$), (E) forelimb stance width ($p = 0.0254$) and (F) gait symmetry ($p = 0.0237$) in TBI mice treated with STING inhibitor (C-176) compared to TBI mice treated with a vehicle. Sham $n = 8$, TBI-vehicle $n = 10$, TBI-C-176 $n = 13$. Data is presented as mean \pm SEM. Significance determined by one-way ANOVA with Tukey's multiple comparison test. * $P < 0.05$, ** $P < 0.01$, *** $P < 0.001$, **** $P < 0.0001$.

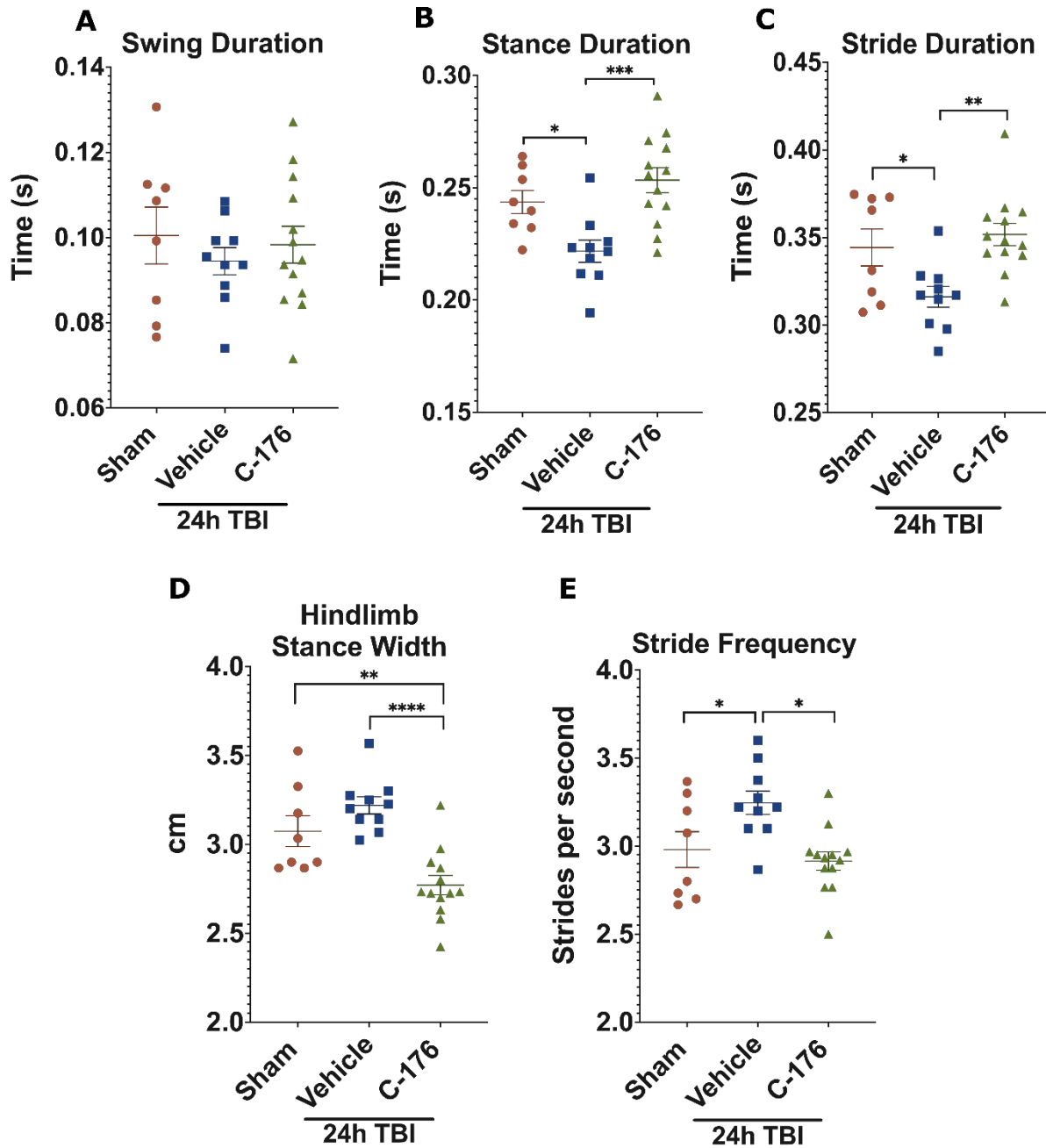


Figure 4. C-176 significantly improves left hindlimb gait deficits 24h post-TBI.

Quantitative temporal gait parameters of mice were measured using DigiGait™ imaging and analysis software 24h after 1.5mm impact CCI surgery (TBI) and no impact (sham). No change in swing duration between treatment groups was observed (A). Significant improvements found in (B) stance ($p=0.0005$) and (C) stride duration ($p=0.0037$), and (E) stride frequency ($p=0.0041$) in TBI mice treated with STING inhibitor (C-176) compared to TBI mice treated a vehicle. (D) Hindlimb stance width in C-176 treated mice significantly lower than sham ($p=0.0052$) and vehicle treated TBI mice ($p<0.0001$). Sham $n = 8$, TBI-vehicle $n = 10$, TBI-C-176 $n = 13$. Data is presented as mean \pm SEM. Significance determined by one-way ANOVA with Tukey's multiple comparison test. * $P<0.05$, ** $P<0.01$, *** $P<0.001$, **** $P<0.0001$

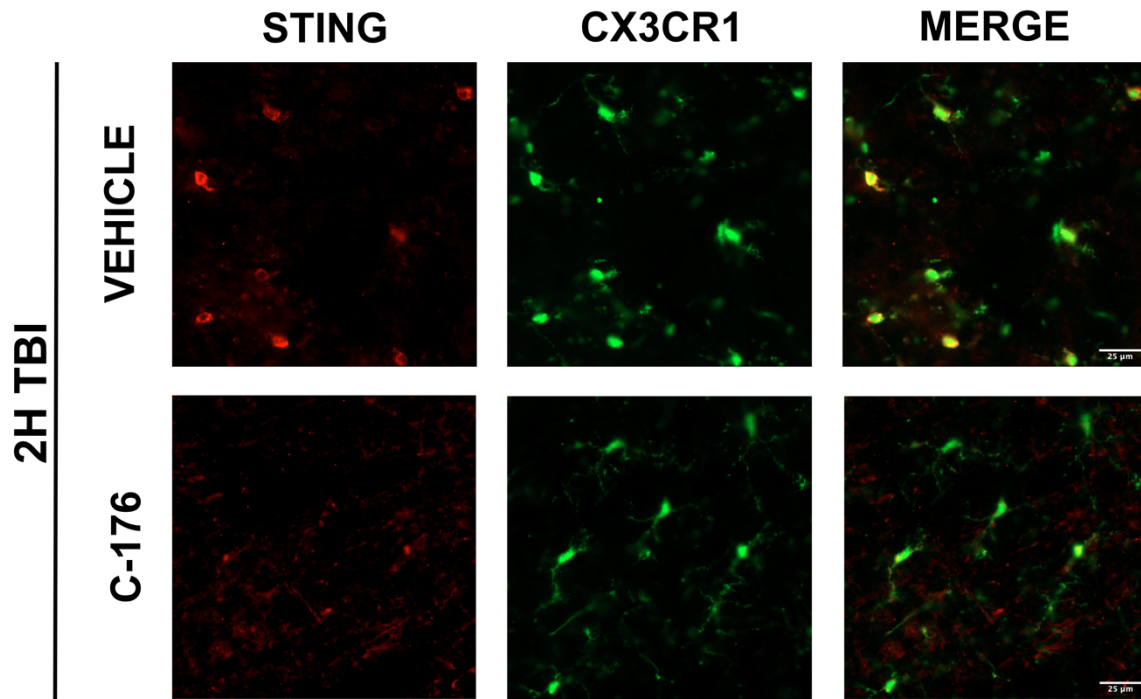


Figure 5. STING expression colocalises with microglia 2h-post TBI.

Representative immunofluorescence images of STING (red) and GFP-tagged CX3CR1 microglia (green) taken around lesion area 2h-post TBI. 30 minutes following TBI, mice were administered a saline vehicle (A) or a single dose of C-176 (B). Images taken on Zeiss Axio Observer 7.1 widefield microscope at 20X objective. Scale bar: 25µm

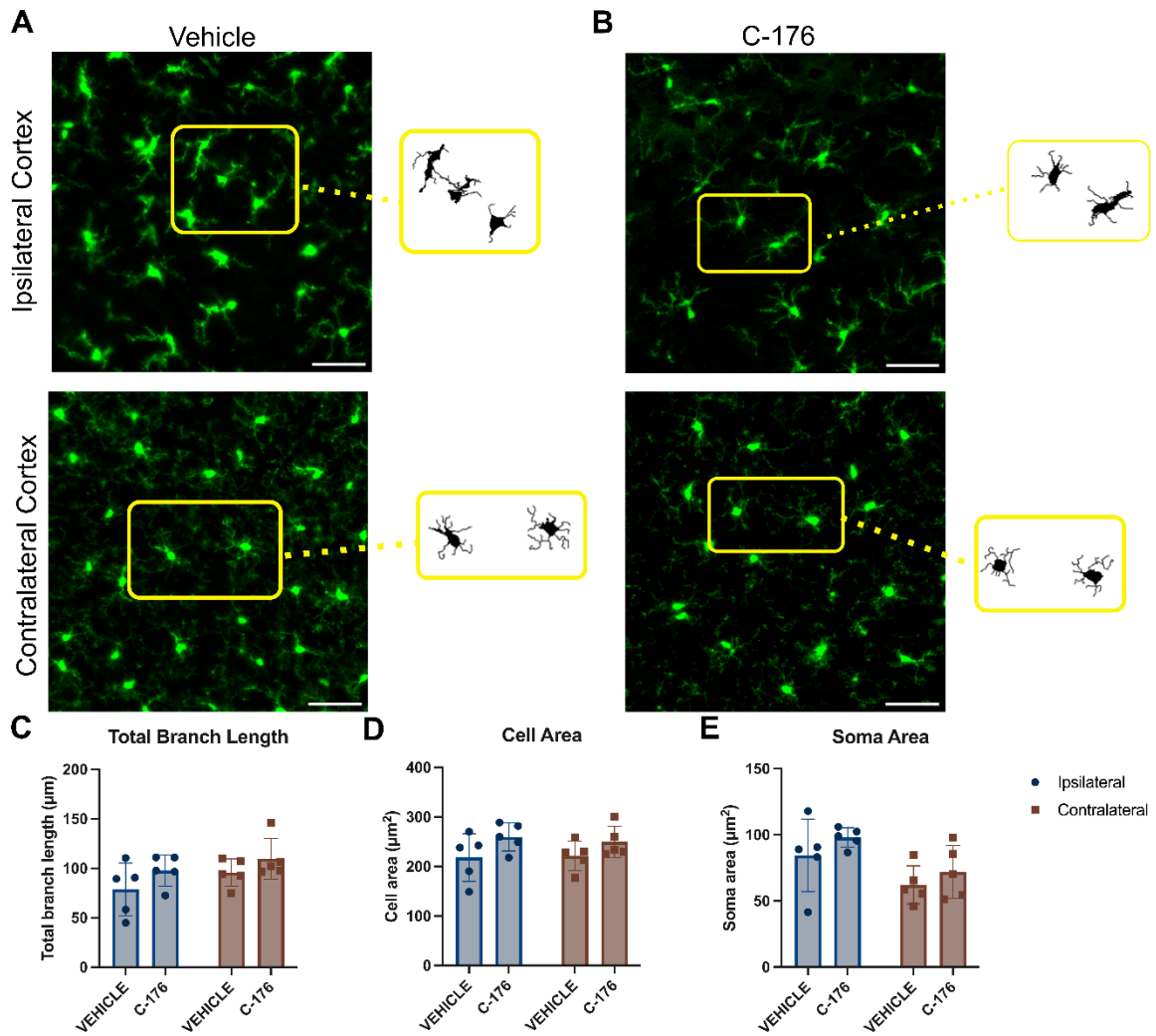
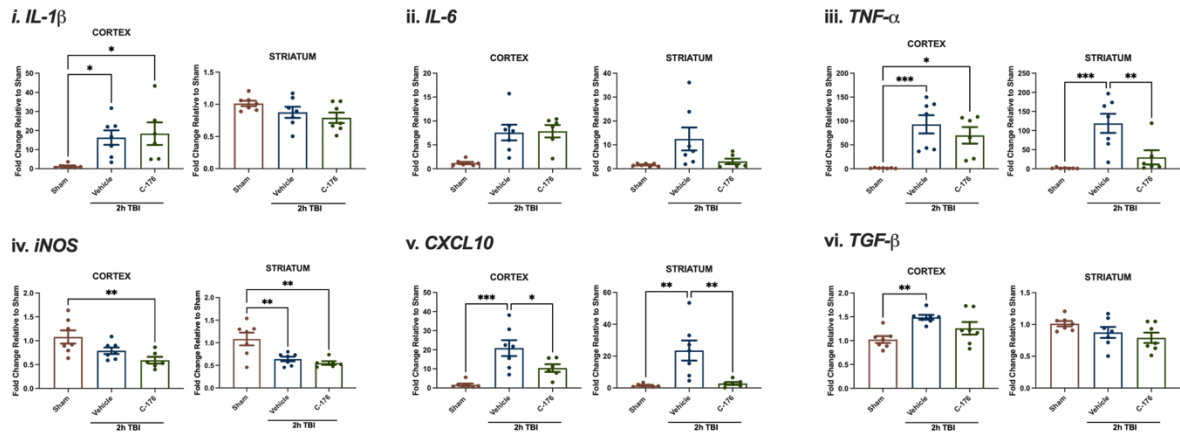


Figure 6. Administration of C-176 does not alter microglial morphology 24h-post TBI.

30µm thick brain sections of CX3CR1^{eGFP} mice subjected to CCI TBI. Representative images are shown for the ipsilateral and contralateral cortex of vehicle-treated (A) and C-176-treated (B) mice with an overview of the skeletonising process employed using a minimum spanning tree algorithm to measure morphological characteristics. Administration of C-176 did not significantly alter (C) total branch length (D), cell area or (E) soma area of perilesional microglia compared to vehicle treated mice 24h-post TBI. Each data point is an average of 200-500 cells. Scale bar = 50µm. n=5 for each group.

A. 2h-post TBI



B. 24h-post TBI

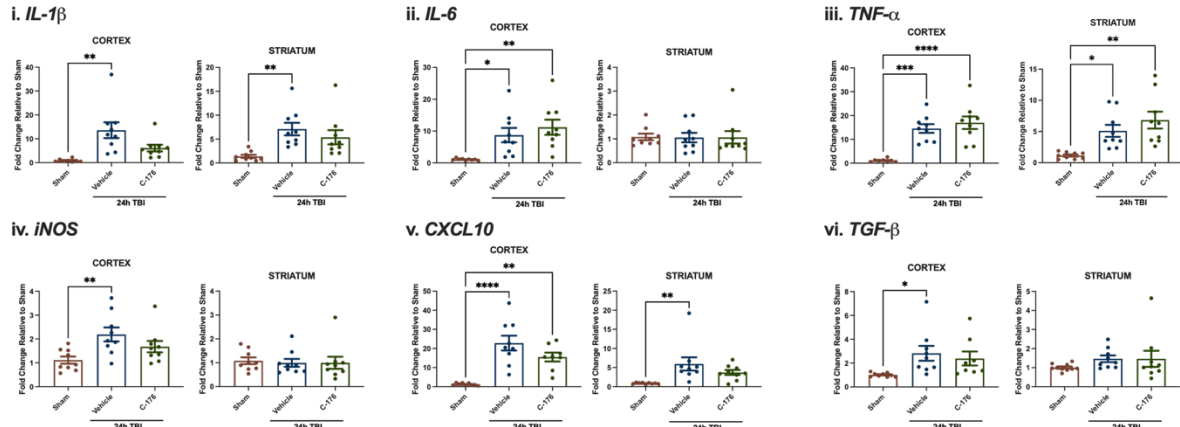
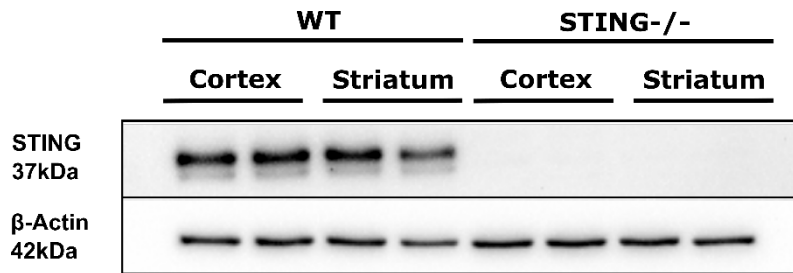


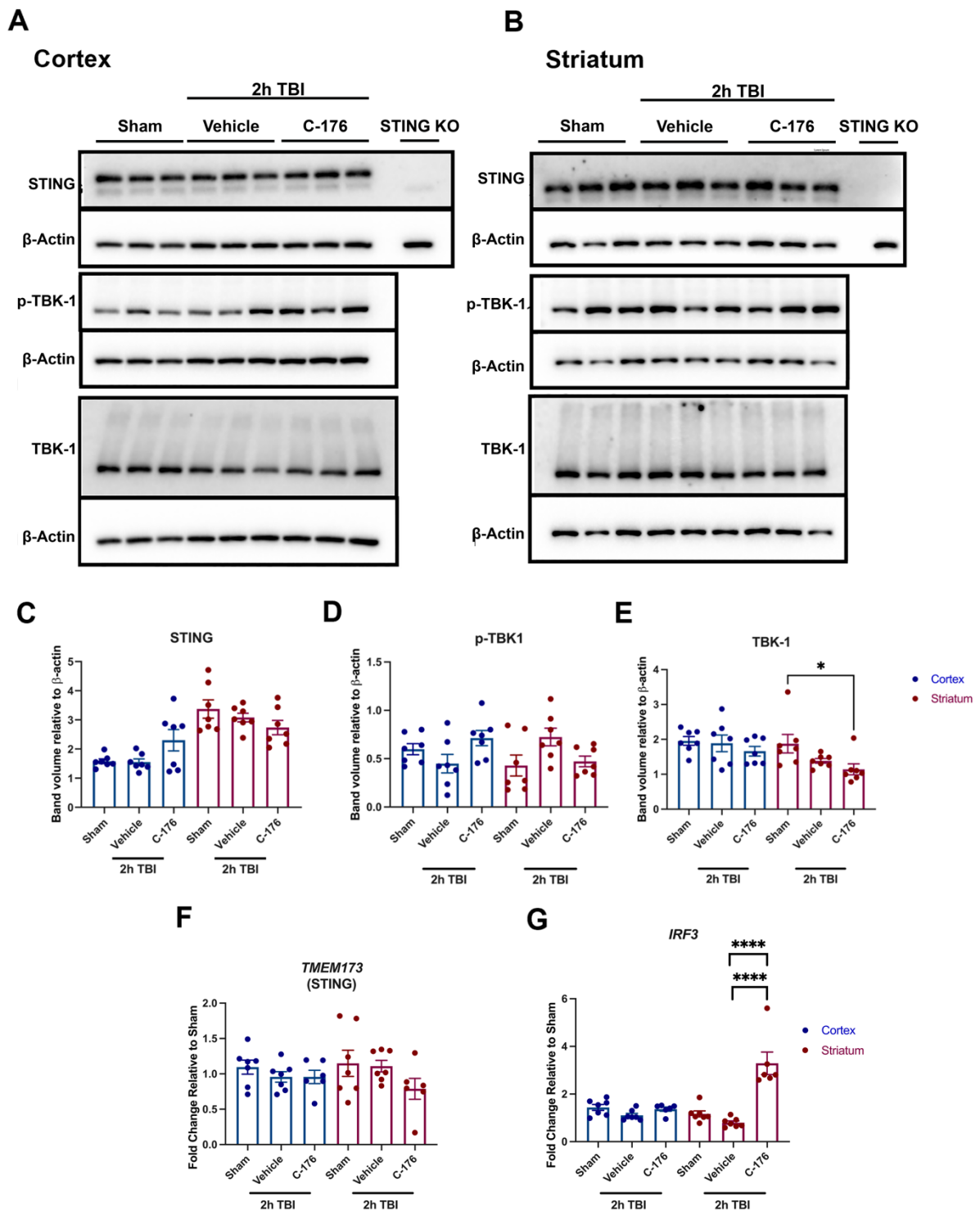
Figure 7. Gene expression of pro-inflammatory markers 2h and 24h following TBI and C-176 administration in mice.

Gene expression as measured by qPCR of pro-inflammatory markers in the ipsilateral cortex and striatum isolated 2h- (A) and 24h-post controlled-cortical impact modelled TBI (B) and intravenous administration with C-176 or a saline vehicle. 2h-post TBI (A), a significant increase in the cortical expression of *IL-1β* (i), *TNF-α* (iii), *CXCL10* (v) and *TGF-β* (vi) was observed. No significant change in the expression of *IL-6* (ii) was found. C-176 treated mice had significant attenuation of *iNOS* expression compared to sham in the cortex and striatum (iv) and significantly reduced expression of *CXCL10* (v) compared to vehicle treated mice in the cortex ($p=0.044$) and striatum ($p=0.0046$). 24h-post TBI (B), vehicle-treated mice increased cortical expression of *IL-1β* (i), *IL-6* (ii), *iNOS* (iv) and *TGF-β* (iii). C-176 treated mice displayed an increase in the expression of *TNF-α* (iii) in the cortex and striatum and *CXCL10* in the cortex (v). All data is presented as mean \pm SEM. 2h-TBI $n=6$, 24h-TBI $n=9$. Significance was determined for the cortex and striatum separately using a one-way ANOVA and Tukey's multiple comparison test. * $p \leq 0.05$, ** $p \leq 0.01$, *** $p \leq 0.001$, **** $p < 0.0001$.



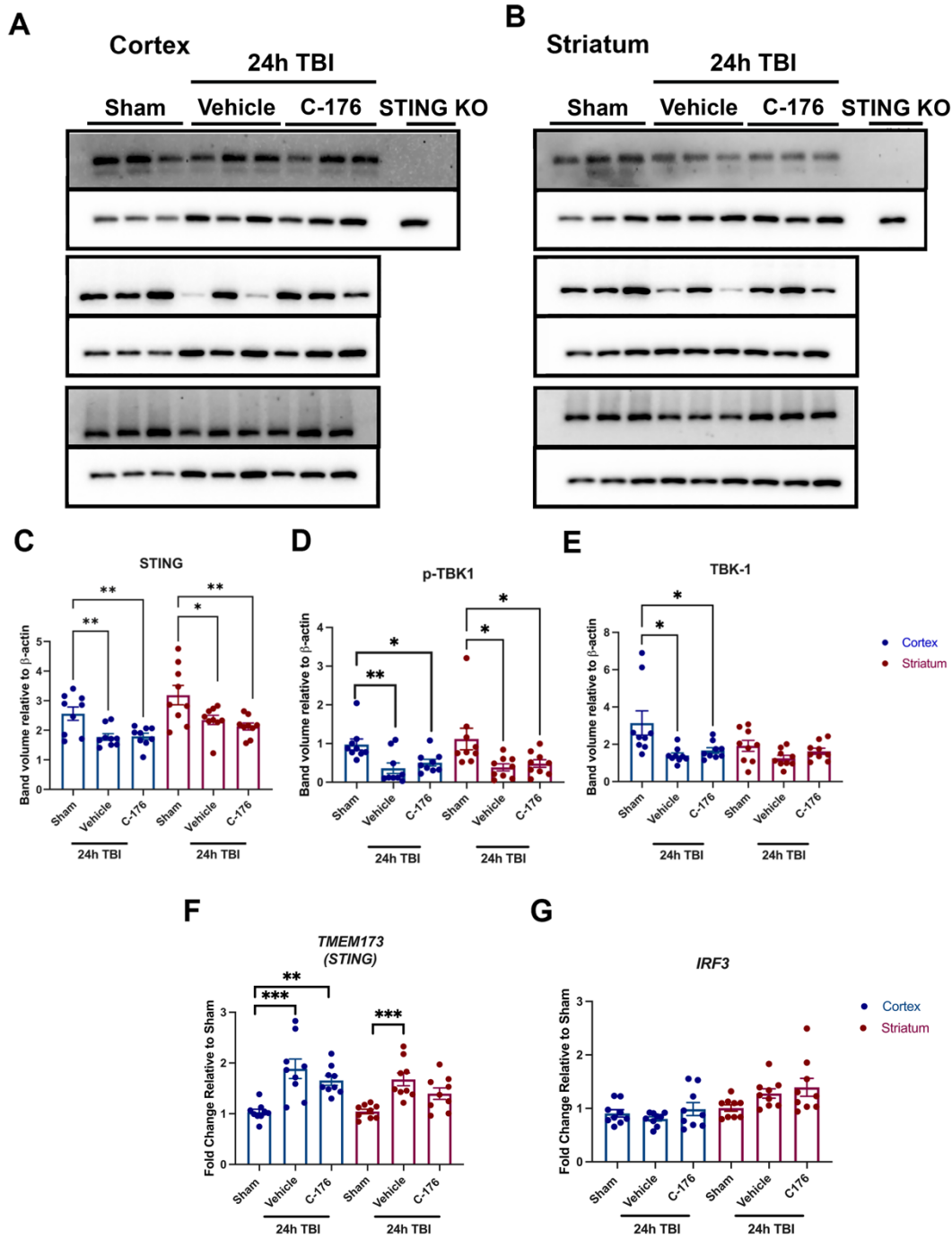
Supplementary figure 1. Validation of STING antibody

Brain lysate extracted from isolated cortex or striatum of wildtype (WT) or STING^{-/-} C57Bl/6 mice. Total STING expression was detected using western blot. A single band was observed at approximately 37kDa in the WT lanes and was absent in STING^{-/-}



Supplementary Figure 2. STING, TBK1 and IRF3 expression 2h post-TBI and C-176 administration.

Representative images of STING, p-TBK1 and TBK1 protein expression the ipsilateral cortex and striatum of mouse brains 2h after controlled-cortical impact modelling of TBI or sham surgery as detected by western blot (A-B). Quantification of total STING (C), phospho-TBK1 (D) and total TBK1 (E) protein expression relative to β -actin loading control. No significant changes in the expression of (C) STING and (D) p-TBK1 were observed following TBI and C-176 administration compared to sham mice. TBI-mice treated with C-176 had a significantly lower expression of (E) total TBK1 compared to sham mice ($p=0.026$). Gene expression analysis by qPCR revealed no significant changes in the expression of TMEM173 (F) in the ipsilateral cortex and striatum and IRF3 (G) in the ipsilateral striatum 2h-post TBI. TBI-mice treated with C-176 had significantly elevated IRF3 expression compared to sham ($p<0.00001$) and vehicle-treated TBI-mice ($p<0.00001$). All data is expressed as mean \pm SEM. Significance determined using a one-way ANOVA with Tukey's multiple comparison test. ** $p \leq 0.01$, *** $p \leq 0.001$. $n = 7$ for each treatment group.



Supplementary Figure 3. STING, TBK1 and IRF3 expression 24h post-TBI and C-176 administration.

Representative images of STING, p-TBK1 and TBK1 protein expression in the ipsilateral cortex and striatum of mouse brains 24h after controlled-cortical impact modelling of TBI or sham surgery as detected by western blot (A-B). Quantification of total STING (C), phospho-TBK1 (D), and total TBK1 (E) protein expression relative to β -actin loading control. Protein expression of STING (C) was significantly decreased in the cortex and striatum of TBI mice treated with vehicle (cortex $p=0.0050$, striatum $p=0.0335$) and C-176-treated mice (cortex $p=0.0062$, striatum $p=0.0064$) when compared to sham mice 24h-post TBI. No significant difference was observed in the expression of STING between the vehicle-treated and the C-176 treated TBI mice. P-TBK1 expression was significantly decreased in the cortex and striatum of both the vehicle-treated (cortex $p=0.0054$, striatum $p=0.0202$) and the C-176 treated mice (cortex $p=0.0350$, striatum $p=0.0480$) compared to sham mice. Gene expression analysis by qPCR revealed an increased expression of TMEM173 (F) 24h-post TBI in the cortex of both the vehicle treated mice ($p=0.0002$) and the C-176 treated mice ($p=0.0057$) compared to sham. Vehicle treated mice also displayed an increased expression of TMEM173 ($p=0.0005$). No significant change in the expression of IRF3 (G) was detected between all treatment groups. All data is expressed as mean \pm SEM. Significance determined using a one-way ANOVA with Tukey's multiple comparison test. ** $p \leq 0.01$, *** $p \leq 0.001$. $n = 9$ for each treatment group.

Table 1. Definition of DigiGait parameters

Gait parameter	Definition	Unit of measurement	Use in mouse models of traumatic brain injury (TBI) or spinal cord injury (SCI)
Swing duration	Time duration of the paw is off the treadmill (swing phase).	Seconds (s)	Ek et al. (2010); Neumann et al. (2009); Sashindranath et al. (2015)
Stance duration	Duration of paw contact with treadmill (stance phase)	Seconds (s)	Neumann et al. (2009); Sashindranath et al. (2015)
Stride duration	Time taken to complete one stride	Seconds (s)	Neumann et al. (2009); Sashindranath et al. (2015)
Stride frequency	The number of strides a paw completes each second. Also known as “cadence”.	Strides per second	Krizsan-Agbas et al. (2014); Sashindranath et al. (2015)
Stance width	The width between the forelimb or hindlimbs at peak stance. Also referred to as “base of support”.	cm	Ek et al. (2010); Krizsan-Agbas et al. (2014)
Gait symmetry	Ratio of forelimb stepping frequency to hind limb stepping frequency. A metric for co-ordination. Healthy mice should have a ratio close to one.	Real #	Krizsan-Agbas et al. (2014)

Supplementary Table 1. Primary antibodies used for western blot analysis

Primary antibody	Host Species	Dilution	Supplier	Catalogue number
STING (<i>in vivo</i>)	Rabbit	1:2000	Abcam	Ab288157
STING (<i>in vitro</i>)	Rabbit	1:1000	Cell Signalling Technologies	13647
Phospho STING	Rabbit	1:1000	Cell Signalling Technologies	72971
Anti-NAK/TBK1	Rabbit	1:1000	Abcam	Ab227182
Anti-NAK/TBK1 (phospho S172)	Rabbit	1:1000	Abcam	Ab109272
Anti-beta actin	Mouse	1:10000	Sigma-Aldrich	A5441

Supplementary Table 2. Secondary antibodies used for western blot analysis

Secondary antibody	Host Species	Dilution	Supplier	Catalogue number
Anti-rabbit immunoglobulins/HRP	Goat	1:1000	Dako Denmark	P0448
Anti-mouse immunoglobulins/HRP	Goat	1:1000	Dako Denmark	P0447

Supplementary Table 3. TaqMan primers used for qPCR analysis

Gene	Species	Refseq	Amplicon size (bp)	TaqMan Assay ID
GAPDH	Mouse	NM_008084.2	107	Mm99999915_m1
TMEM173 (STING)	Mouse	NM_028261.1	173	Mm0115817_m1
TNF α	Mouse	NM_013693.3	81	Mm00443258_m1
IRF3	Mouse	NM_016849.4	59	Mm00516779_m1
IL-6	Mouse	NM_031168.1	78	Mm00446190_m1
IL-1 β	Mouse	NM_008361.3	63	Mm01336189_m1
CXCL10	Mouse	NM_021274.2	59	Mm00445235_m1

Supplementary Table 4. SYBR primers used for qPCR analysis

Gene	Forward primer (5'3')	Reverse primer (5'3')
GAPDH	ATCTTCTTGTGCAGTGCCAGC	ACTCCACGACATACTCAGCACC
iNOS	CAAGCACCTTGGAAGAGGAG	AAGGCCAAACACAGCATACC

Supplementary Table 5. Primary antibodies used for immunohistochemistry

Primary antibody	Host Species	Dilution	Supplier	Catalogue number
STING	Rabbit	1:500	Novus Biologicals	NBP2-24683

Supplementary Table 6. Secondary antibodies used for immunohistochemistry

Secondary antibody	Conjugate	Dilution	Supplier	Catalogue number
Goat anti-rabbit IgG	Alexa Fluor 594	1:1000	Invitrogen	A-11012